Journal of Applied Sciences

ISSN 1812-5654

science alert

ANSInet
an open access publisher
http://ansinet.com

Journal of Applied Sciences 14 (10): 1078-1082, 2014
ISSN 1812-5654 / DOI: 10.3923/jas.2014.1078.1082
© 2014 Asian Network for Scientific Information

Fundamentals of Marine Propeller Analysis

Kiam Beng Yeo and Wen Yee Hau
Unit Kajian Bahan dan Mineral, Sekolah Kejuruteraan dan Teknologi Maklumat,
Universiti Malaysia Sabah, Jalan UMS, Kota Kinabalu, 88400, Sabah, Malaysia

Abstract: This study illustrates the fundamentals of marine propeller analysis through the importance of hydrofoil geometry. Propeller geometries are being described initially with its solid mechanics, followed by flow interaction between solid-fluid in the hydromechanics environment. Hydrofoil analysis in two-dimension is correlated with solid propeller geometries and demonstrated. The solid mechanics of marine propeller that converted its resultant forces and moments to flow hydrodynamics is also described by a summarization of theories from the evolving foundation of the analytical work in the field of marine propeller.

Key words: Marine propeller, hydrofoil, hydrodynamics

INTRODUCTION

Evolution of commercial marine propeller that was widely used in the current market comes from the propulsion design concept by Robert Hooke for his watermill design principle to gain energy from the dynamic mechanism. Archimedean screw was implemented in propeller mechanism and Joseph Bramah was the inventor of screw type propulsion system for the stern of the ship (Carlton, 2007). Methods that were used to predict the hydrodynamic flow characteristics for various geometries included the computational and experimental approaches for propeller performance analysis. However, enhancement of theoretical analysis is continuously improved to coherently and effectively implement in the geometric design of marine.

Analysis of propeller geometries started from two-dimensional hydrofoil with resultant forces and moments, followed by three-dimensional marine propeller that could best predict the performance in solid-fluid interaction. Nevertheless, predicting of flow in three-dimensional analysis being much more complicated due to its nonlinear flow behavior caused by the ship hull and wave effect (Subhas *et al*., 2012). More precise and accurate ways in analytical methods are required to predict the geometric performance with changes of parameters.

TWO-DIMENSIONAL HYDROFOIL GEOMETRY

Similar to airfoil development, hydrofoil analysis with varied angle of attack is studied for optimizing the lift to drag ratio to identify the performance characteristics in hydrodynamic flow interaction. Basic formation of propeller blade is developed through different hydrofoil section analysis from root to tip. The hydrofoil blade is designed to effect the pressurizing of both suction and pressure surfaces to produce the resultant lift and drag on each foil element which generates the required net lift of the hydrofoil blade to drive the propeller.

The thickness of the geometric blade section also underlines the analytical outcome. For a strong material, hub to tip section in hydrofoil could remain constant but in commercialized design of marine propeller, root thickness is increased to improve its strength in supporting the resultant force distribution over the surface area. Fine pitch on hub and coarse pitch setting on tip is an attempt to produce as efficient as possible the thrust force over the entire span area. In purpose, the twisted blade is not to maintain the angle of attack, where the pitch angle varies along the blade references line.

When propeller rotates, the root section of the hydrofoil suffers lesser mass flow rate but the tip section overcomes a much higher fraction as the sectional radial ratio increased. Higher lifting force is built for the hydrofoil closed to the tip section but a higher drag force occurs on the hydrofoil which is closed to the root section and exceeding its optimum attack angle. Figure 1 showed the resultant forces on the hydrofoil section. Equation 1 and 2 expressed the summation of resultant forces on every element of the hydrofoil that contributes to the total drag and lift forces:

$$\sum_{n=1}^{k} F_D = \begin{bmatrix} (F_{Pressure} + F_{Tangential\ shear} + F_{Induced})_{n=1} + \cdots \\ +(F_{Pressure} + F_{Tangential\ shear} + F_{Induced})_{n=k} \end{bmatrix} \quad (1)$$

Corresponding Author: Kiam Beng Yeo, Unit Kajian Bahan dan Mineral, Sekolah Kejuruteraan dan Teknologi Maklumat, Universiti Malaysia Sabah, Jalan UMS, Kota Kinabalu, 88400, Sabah, Malaysia
Tel: +6088320000, Ext: 3236

$$\sum_{n=1}^{k} F_D = \begin{bmatrix} (F_{Pressure} + F_{Normal\ shear} + F_{Induced})_{n=1} + \cdots \\ +(F_{Pressure} + F_{Normal\ shear} + F_{Induced})_{n=k} \end{bmatrix} \quad (2)$$

For the drag force of hydrofoil, pressure drag is the drag force caused by pressure of fluid flow; skin friction drag being the shear stress acting on the foil that induced drag is produced by parallel stream flow. While, the lift force of the hydrofoil has a normal shear compare to tangential shear stress as drag component acting on the foil surface.

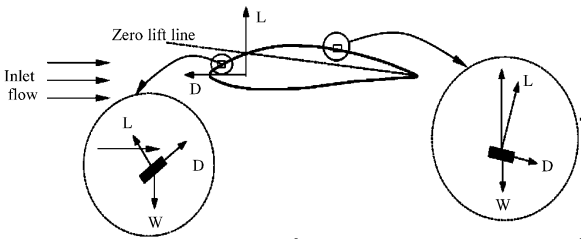

Fig. 1: Resultant forces of hydrofoil

Flow characteristics of hydrofoil section: Flow interaction of hydrofoil at low rotational motion displayed behaviors of flow characteristics as in Fig. 2. Vortex starting to form from the hub section of the foil section and grows larger as it goes nearer to the tip section; low rotation induced vortex dies off close to surface of hydrofoil. Nevertheless, high rotational motion will not produce vortex closed to the blade surface due to high kinetics that pull the vortex with higher speed. Flow behaviors of high rotational motion propeller with flow interaction are also displayed in Fig. 3.

For propeller geometry design, the hydrofoil thickness of the propeller blade becomes thinner as it crossed from the root to the tip section. The root section shall be thicker as higher stress is induced by the hydrodynamics forces requires a larger area to support the whole force distribution on the blade surface. In hydrofoil design, propeller is twisted from its hub to tip to produce increment of angle of attack is manufactured in a smooth finishing to yield constant thrust needed by the propulsion.

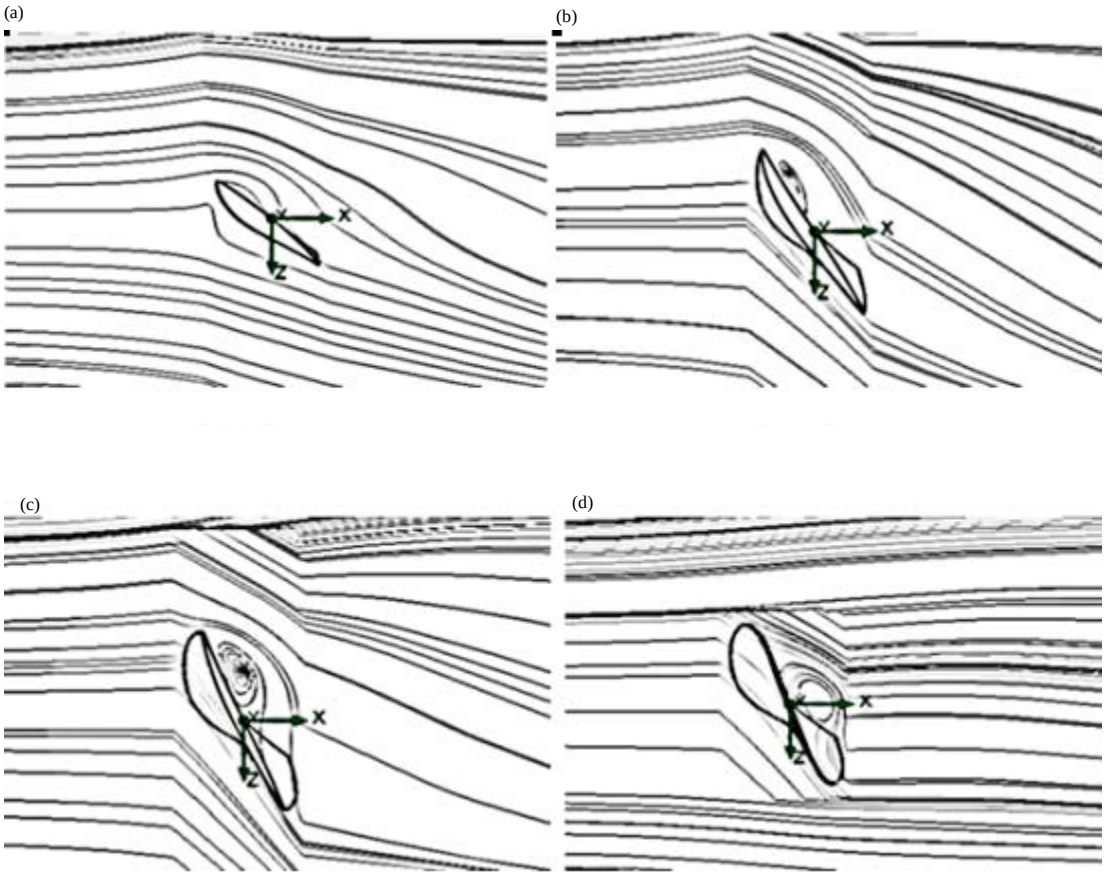

Fig. 2(a-d): Low RPM flow interaction of different sectional radius, r/R ration of (a) 0.3, (b) 0.5, (c) 0.7 and (d) 0.9

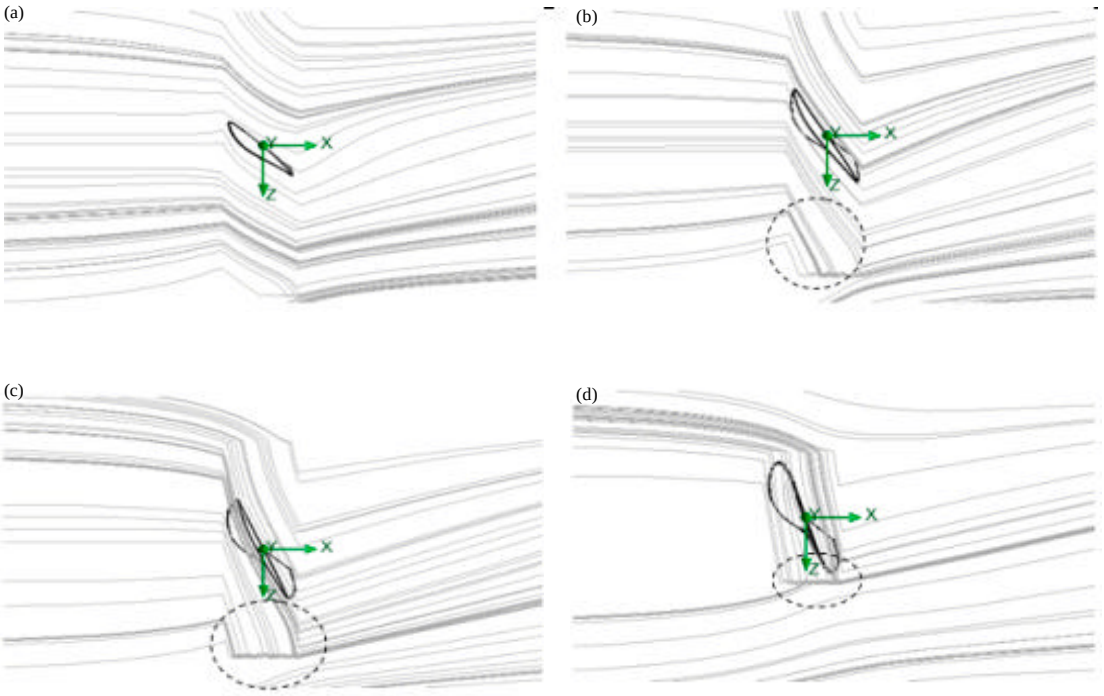

Fig. 3(a-d): High RPM flow interaction of different sectional radius, r/R ration of (a) 0.3, (b) 0.5, (c) 0.7 and (d) 0.9

Figure 4 displays the pressure distribution over the hydrofoil section that occurred in solid-fluid interaction. From point 1, flow separation occurs on the upper layer of the suction surface and the lower layer for pressure surface. As the fluid flow from point 1 to 2, the reduction of positive pressure distribution takes place with higher fraction of pressure at the suction surface compared to suction region. As the flow moves from point 2 to 3, pressure reduced to extremely low until negative pressure value at point 3. From point 1 to 3, small reduction of pressure over the pressure surface also occurred. For the changes of hydrofoil from hub to tip section, the pressure differences become very large which also complies to the Bernoulli's theorem as it rotates with varying speeds.

When the attack angle starts to increase as in Fig. 5, surface of regions A to B on the suction surface achieves reduction of pressure and the characteristics over this region is a laminar flow. Continuous reduction of pressure occurred until region C where adverse pressure gradient starts to take place. This region has steadily separated from point C that starts to break off from the propeller surface or boundary layer due to interaction of higher shear and viscosity effect.

Right after the downstream of the transition of flow separation, the entire boundary layer and flow field becomes highly turbulent as in the after region D. When

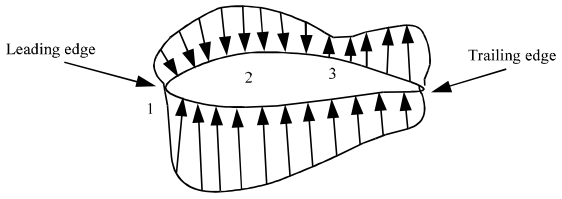

Fig. 4: Pressure distribution of marine propeller hydrofoil

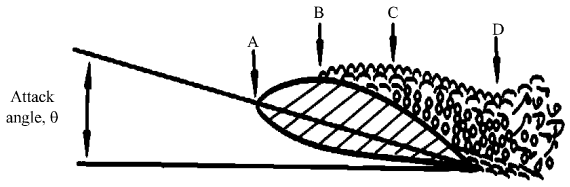

Fig. 5: Higher attack angle of flow characteristic profile

highly adverse pressure gradient at downstream area becomes large enough, the boundary streamlines would break away from the hydrofoil surface. The effect of this phenomenon produces high turbulence and kinetic energy flow that pressurized the trailing edge with unsteady pressure.

Elevation of attack angle produces premature of flow separation earlier than required, at region after point C.

This breakoff would break apart faster than required for resultant lift force due to occurrence of stall. For premature of flow separation or high angle of attack, high drag force would occur at the hydrofoil (Carlton, 2007). As the hydrofoil gets closer to the tip section, higher lift force with thin section that has higher flow pressure differences and occurrences of low to high pressure induces cavitation.

Resultant forces and moments on propeller: For basic modeling of marine propeller, simple formation and analysis of hydrofoil that described the forces and moments interaction shall be considered. Earlier design of general marine propeller structure is described by the rotational motion of propeller blades with simple mechanics (Fig. 6) for the solid body as it rotates about the hub center about the x-axis.

However, this analysis does not predict the wake field that emerged non-linearly. As propeller rotates about its center of the hub axis, each blade suffers different inflow field effect which caused various amplitude of cyclic change in its resultant moments and forces. When propeller blade rotates in the wake field, cyclic lift forces generated by rotating mechanism would pull and push as much water as possible for the forward thrust, the resultant thrust and torsional which could be derived by mean and harmonic components of these forces as described in Eq. 3 and 4:

$$F(t) = F_0 + \sum_{n=1}^{k} F_n \cos(\omega t + \phi_n) \quad (3)$$

$$M(t) = M_0 + \sum_{n=1}^{k} M_n \cos(\omega t + \phi_n) \quad (4)$$

Pressure loading with changes of coordinates: Pressure loading on the marine propeller blade changes from coordinate to coordinate as it moves with rotational motion. For the force changes of coordinate on the propeller body, it is convenient to analyze the element with cylindrical coordinate system. Figure 7 shows the element position with the coordinate changes on the three dimensional propeller blades for the blade loading in uniform flow analysis (Breslin and Andersen, 1996). Equation 5 and 6 shows the relationship for axial and tangential forces with element changes:

$$Fa' = -\frac{\Delta p(h', r')}{r} \cos\alpha.\ \delta(r - r').\ \delta(x - x').\ \delta(\theta - \theta')\, ds' \quad (5)$$

$$Ft' = -\frac{\Delta p(h', r')}{r} \sin\alpha.\ \delta(r - r').\ \delta(x - x').\ \delta(\theta - \theta')\, ds' \quad (6)$$

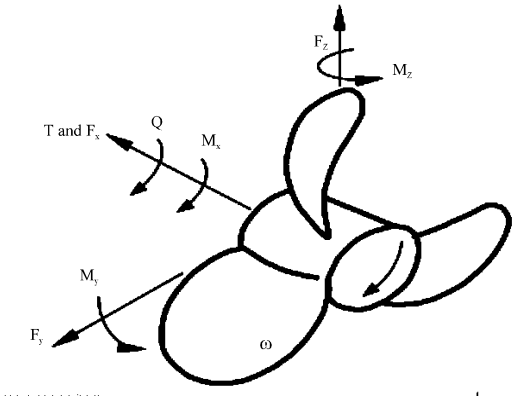

Fig. 6: Forces and moments for marine propeller

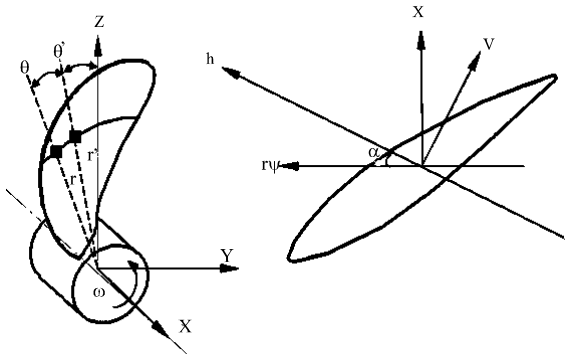

Fig. 7: Changes of cylindrical coordinates on marine propeller

Developed analytical methods: The first ever analytical theory of marine propeller was proposed by Rankine and refined by Froude. The momentum theory was the oldest method to define the producing thrust of a propeller. Rough estimation about an ideal fluid for working condition, disc assumption for blade numbers and thrust with the obtained velocity from fluid streamlines are considered. By improvement to the momentum theorem, Froude developed the analytical method that further describes the thrust and torque of the propeller by correlating the geometry shape of propeller blade as well as hydrofoil shape through integration of blade element that has different sectional radial for a proper thrust and torque of the propeller body.

Blade element theory provides a better assumption on the mechanics basis direct to the hydrofoil. Formation of lift and drag forces with respect to changes of blade radius is as shown in Eq. 7 and 8. Figure 8 shows the analysis details related to the theory while thrust and torque estimation is shown in Eq. 9 and 10 (Molland, 1992). From the basic hydrofoil shape, drag-D and lift-L

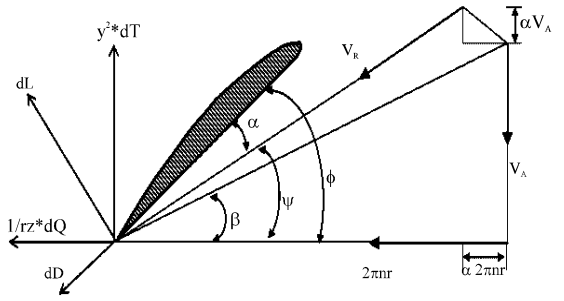

Fig. 8: Blade element theory with induced velocities (hydrofoil section)

forces are hence investigated and implemented to obtain the torque and thrust loadings:

$$dL = 0.5C_L\rho c dr V_R^2 \quad (7)$$

$$dD = 0.5C_D\rho c dr V_R^2 \quad (8)$$

$$dT = 0.5zC_L\rho c dr V_R^2 \cos\beta\,(1-\tan\beta\tan\gamma) \quad (9)$$

$$dQ = 0.5zC_L\rho c dr V_R^2 \cos\beta\,(\tan\beta+\tan\gamma) \quad (10)$$

CONCLUSION

The marine propeller geometry is formed by two-dimensional hydrofoils that developed a very simple foundation of flow interaction before complex three-dimensional analyses need to concern. Rotational motion of marine propeller in its hydromechanics allows increment of kinetic energy of the fluid flow that it pulls and pushes. This mechanism produces the required thrust to propel the whole propulsion as well as the ship for its forward movement.

The solid propeller mechanics transform its forces to the fluid dynamics environment when the propeller rotates to fulfill the law of conservation of mass. Current trend of analytical work on propeller has moved towards the Reynolds Averaged Navier Stoke equation with the aided of computational analysis due to many advantages in predicting propeller and flow behaviors which involved the fluid characteristics in laminar, transition and turbulence effect for various interaction of solid with fluid motion. As the propeller rotates, different pressures, forces and moment loading would occur on the blades body which produces different stress loading and eventually affect the whole formation and designation of the propeller geometries.

ACKNOWLEDGMENT

The authors would like to express their appreciation to the Unit Kajan Bahan dan Mineral (Materials and Minerals Research Unit), School of Engineering and Information Technology, Universiti Malaysia Sabah and the Ministry of Higher Education of Malaysia for their support.

NOMENCLATURE

α = Attack Angle
β = Pitch Angle without Induced Velocities
c = Chord Length
C_D = Drag Coefficient
C_L = Lift Coefficient
D = Drag
F_D = Drag Force
F_L = Lift Force
L = Lift
P = Pressure
ρ = Density
Q = Torque
r = Radial
T = Thrust
t = Time
V_A = Axial Velocity
ω = Angular Velocity
ϕ = Angular Displacement
θ = Azimuth

REFERENCES

Breslin, J.P. and P. Andersen, 1996. Hydrodynamics of Ship Propellers. Cambridge University Press, Cambridge, UK., ISBN-13: 9780521574709, Pages: 559.

Carlton, J.S., 2007. Marine Propellers and Propulsion. 2nd Edn. butterworth-Heinemann, Oxford, UK.

Molland, A.F., 1992. The prediction of rudder-propeller interactions using blade element-momentum theory and modified lifting line theory. Ship Science Reports, University of Southampton, Southampton, UK.

Subhas, S., V.F. Saji, S. Ramakrishna and H.N. Das, 2012. CFD analysis of a propeller flow and cavitation. Int. J. Comput. Appl., 55: 26-33.